Indian J. Phys **80** (7), 727-736 (2006)

IJP

Monte Carlo simulation of electron transport in metallic and biological materials

M F Rahimi[1] and N Ghal-Eh[2]*

[1]Physics Department, School of Sciences, Ferdowsi University of Mashhad, Mashhad, Iran

[2]Physics Department, Damghan University of Basic Sciences, Damghan, Iran

E-mail ghal-eh@dubs.ac.ir

Received 2 November 2005 accepted 11 May 2006

Abstract : A simple Monte Carlo procedure is described for simulating the multiple scattering and absorption of electrons with definite incident energy in the range of keV up to 20 MeV, moving perpendicular or at a definite angle through one slab, or two adjacent slabs of uniformly-distributed material of given atomic number, density and thickness The simulation is based on a Screened Rutherford ion and Bethe continuous energy-loss equation Programs were written in FORTRAN to determine scattering, backscattering, and absorption coefficients, providing the user with a graphical output of the electron trajectories The results of several mulations are presented by using various numbers of electrons The program is used to analyze the relation between the energy and the nge of electron in the slab, the scattering, backscattering, absorption, transmission coefficients and the angular distribution The chnique has been applied to the transport properties of the electron through body tissue, bone and water slab by dividing media into several parts of different materials Comparisons show that the results are in good agreement with the MCNP code within the range of energy considered and with the experimental data of Linear Electron Accelerator of Imam-Reza Hospital in Mashhad, Iran

Keywords : Electron transport, Monte Carlo simulation, electron linear accelerator, MCNP code, biological materials

PACS Nos : 02 70 Uu, 61 43 Bn, 87 53 Wz

1. Monte Carlo method

The Monte Carlo is a numerical method for simulating complex statistical (*e g* particle transport) or non-statistical (*e g* integration) problems. When we are dealing with multi-parameter problems or those in which there is not an analytical solution, this method has been used frequently [1] The main idea is to propose a statistical model, which is compatible with the problem or the problem is simulated exactly The construction of random parameters is based on particular rules from which the phenomenon is sampling several times.

The advantage of this method is the ability of solving complex problems and the main disadvantage is having a huge number of computations and consequently, a long run-time of computer program, namely, to increase one digit to our result, the time consumption increases hundred times.

*Corresponding Author

The random number is between 0 and 1, and it is used in all interactions to determine which kind of interactions (absorption, elastic scattering, *etc.*) takes place, how much energy is lost, what the direction of the particle is (in scattering), *etc.*

In this section, a brief basic description of the Monte Carlo method will be given The following description gives the method of sampling of a collision along a track The free path length L of an electron (*i.e* distance between successive collisions) is a random variable. The probability $p(L)dL$ of occurrence of a collision between L and $L + dL$ along its path is :

$$p(L)\,dL = e^{-\sigma_t L}\sigma_t dL, \tag{1}$$

where

$$\sigma_t = \sum_i^n N_i \sigma_i , \tag{2}$$

σ_t = the total macroscopic cross section, or the probability of interaction in the unit length of the particle path

N_i = number of atoms per unit volume

σ_i = the differential cross section

Now, suppose a random number as ξ in the interval of (0,1).

$$\xi = \int_0^L e^{-\sigma_t S} \sigma_t dS = 1 - e^{-\sigma_t L} \tag{3}$$

It then follows that

$$L = -\frac{1}{\sigma_t} \ln(1 - \xi). \tag{4}$$

But, as $(1 - \xi)$ is distributed in the same interval as ξ, it may be replaced by (ξ) Then we obtain a well-known expression for the distance between collisions

$$L = -\frac{1}{\sigma_t} \ln(\xi) \tag{5}$$

The total macroscopic cross section is

$$\sigma_t = \sigma_a + \sigma_s, \tag{6}$$

where σ_a and σ_s are the macroscopic absorption and scattering cross sections, respectively; then (σ_s/σ_t) indicates the probability of scattering while (σ_a/σ_t) represents the probability of absorption Now, having produced the random number ξ, the program can determine the kind of interaction that one interacting electron undergoes

If $(\sigma_a/\sigma_t) < \xi < 1$, we suppose that a scattering interaction could take place, and if $0 > \xi > (\sigma_a/\sigma_t)$ then an absorption interaction occurs.

In order to determine the interacting atom with the random number ξ within interval (0,1), the k-th atom is chosen as the collision atom In this case, $p_{k-1} < \xi < p_k$ where $p_k = (\sigma_k/\sigma_{tot})$

The angles and the energies of the incoming electrons after collisions are determined similarly. The cosine of the scattering angle is sampled from energy-dependent angular distribution formula for each collision

2. Physics of electron interactions with matter

The transport and penetration of electrons in matter in the energy range of interest involve interactions which result either in direct energy losses or scattering, or a combination of both The most important interactions include elastic nuclear scattering off a nucleus (Coulomb scattering), inelastic interactions with orbital electrons and radiative collisions with both nuclei and orbital electrons The mode of interaction is largely determined by the energy of the passing electron and the distance of electron approach to the atom (or nucleus) with which it interacts (called impact parameter)

2.1 *Energy losses of electron*

Collisions which lead to direct energy loss by passing electron are of primary interest, since such events give rise to direct deposition of energy, and hence an absorbed dose In the irradiated medium, the energy losses usually take place in small increments, and an electron must therefore suffer many collisions before it loses all its energy A 10 MeV electron will undergo some 100000 interactions before coming to rest Two principally different energy loss processes may occur (a) Collision losses and (b) Radiation losses. The fundamental difference between the above processes is that the collision loss involves the outer atomic electrons, while the radiation losses involve the atomic nucleus [2].

2.1.1 *Collision losses*

The electron may suffer collisional energy-loss in either of two processes atomic excitation and ionization The probability for a given type of collision depends upon the energy of the passing electron and the atomic number of the medium in which the collision takes place If the closest approach to the atom of the passing electron is large compared with the dimension of the atom, the atom responds as a whole to the variable force exerted upon it by the passing electron Such an interaction results in an excitation of the atom. For these relatively distant collisions, the magnetic force is of secondary importance, since it varies inversely proportional to the third power of the distance, whereas the Coulomb force varies inversely proportional to the square of distance. During the excitation, an electron from an inner shell is moved to an outer orbit The energy required to do this is only a few eV and consequently, the energy loss of the impinging electron is small. The excited atom dissipates the excess energy by emitting visible radiation if the medium is a gas, whilst in a solid material, the excess energy is imparted to the medium in the form of heat.

The cross section for the excitation and ionization type of collisions is large. For energies of the order of a few MeV, these are the major mechanisms of energy degradation experienced by electron beams. It is because

of the almost continuous loss of energy in multiple interactions of this type that the primary electron beam has an almost precise range in a medium.

2.1.2 *Radiation losses*

The energy lost by the electron into radiation is high if the distance of the electron's closest approach to the atom is smaller than the atomic radius. If this happens, the incident electron will, under the influence of the nuclear Coulomb field, be deflected from its trajectory with a loss of energy. The loss of energy will be emitted in the form of electromagnetic radiation, known as Bremsstrahlung. This is a fundamental process for production of continues X-rays with energy up to maximum kinetic energy of the passing electron. This collision results in the production of electromagnetic radiation and the deflection of the incident electron from its original path. At high energy, the phenomena accompanying the Bremsstrahlung production are quite complicated. The energy loss due to the production of Bremsstrahlung photons of frequency ν per electron path length dx is given by

$$\frac{dE}{dx} = 4Z^2 \frac{N}{137} r_e^2 h\nu_{max} \frac{183}{Z^{1/3}} \tag{7}$$

where Z is the atomic number, N is the number of nuclei per unit volume of material, r_e is the classical radius of the electron, h is Plank's constant, and ν is the frequency of the Bremsstrahlung. This expression is approximate and valid for energy $E >> mc^2Z^{1/3}$, i.e. for the case where the screening of the nucleus by the outer electrons is taken into account. The angular distribution of the Bremsstrahlung is of importance. For low incident electron energy ($E<<mc^2$), the maximum intensity is in the direction perpendicular to the direction of the electron motion. At very high energy ($E>>mc^2$), the average angle of the quantum emission relative to the incident electron is $\theta = mc^2/E$, and is thus independent of the energy of the emitted photons.

The rate of the energy loss by a radiation collision per atom is proportional to Z^2, and per electron $\approx Z$. Thus, compared to the water of $Z \approx 7.42$, the radiation loss Z_h in any higher atomic number material will be larger by a factor of $Z_h/7.42$. Consequently, energy loss per gram per square cm depends on Z. In addition, Bremsstrahlung production with the atomic electron (not nuclear field) is also possible. While the electron-nucleus Bremsstrahlung proportional to Z^2, but the electron-electron Bremsstrahlung to Z. The latter effect is therefore only important for low Z material and at extreme relativistic energies.

Another form of electromagnetic radiation emission during a passage of electrons through a medium is the Čerenkov light. This effect is the result of electrical polarization of the insulate medium which occurs during the passage of relativistic electrons. The depolarization of target molecules causes the emission of visible light along its path. The effect is appreciable only for relativistic velocities, but not more than a few percents.

2.2 *Stopping power*

Information about the manner in which the charged particles, such as electrons, lose their energy along their tracks during the passage through matter, is presented in the form of a quantity called stopping power. The linear stopping power is defined as dE/dl, or dT/dx, where dE or dT is the fraction of energy which an electron loses during its passage through a medium along an increment of path dl or dx. In many applications, a Mass Stopping Power is used by relating dE/dl to the physical density of target ρ. With the stopping power S in MeV cm^{-1}, conversion to (S/ρ), in MeV g^{-1} cm^{-2} is done by density in g cm^{-3}. We have to consider separately the collision stopping power due to inelastic collisions with atomic electrons of the medium resulting in excitations and ionizations, and the radiation stopping power due to the electron interaction with the electric field of the nucleus resulting in the production of Bremsstrahlung, and then evaluate the Total Mass Stopping Power of the medium [3]. Figure 1 shows the relative contribution of the

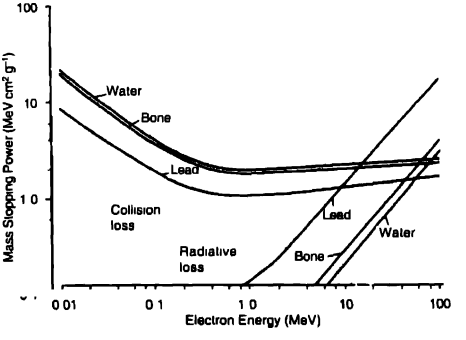

Figure 1. Relative contributions of the collisional and radiative losses for water, bone and lead, for a wide range of electron beam energies

collisional and radiative losses for water, bone and lead, for a wide range of electron beam energies. It is seen that collisional losses are dominant in the low energy range, and the radiative losses becoming of comparable magnitude at about 10 MeV for high Z materials. In contrast with collisional losses, which show a minimum between 1 and 2 MeV, radiative losses increase linearly with electron energy.

2.3 *Scattering processes*

Another important aspect of electron interactions with atoms, apart from energy losses, is the change in the direction of the electron motion leading to scattering. Electron scattering plays an important role within and at the homogeneity boundaries, strongly affecting the local dose distribution, which may lead to serious distribution distortion and even over dosage. One has to distinguish between single and multiple scattering processes. Single scattering results in a large angular deflection of the electron, whereas small-angle deflections are associated with multiple scattering. The intermediate case is known as plural scattering. Two interaction processes are particularly important in scattering: interactions of the passing electron with the Coulomb field of the nucleus, and electron-electron collisions. These two scattering cross sections are both large and pointed in the forward direction, resulting in a large number of small-angle scattering , the all dis in the medium. If these interactions involve an atomic electron, a secondary knock-on (delta ray) electron may be produced and a significant part of the passing electron energy can be transferred to the target. Scattering in the nuclear Coulomb field involves, in most cases, a negligible energy transfer, since the mass of the target nucleus is so much greater than that of the electron.

2.4 *Backscattering*

When a beam of electrons impinges on a solid target, most of the electrons penetrate into the target, but a proportion of them returns back to the surface and escape into space. Most of incident electrons suffered elastic or inelastic collisions or both and were backscattered 'Up-Stream' towards the source of the primary beam.

It has been established, in the experimental studies of backscattering carried out so far, that the intensity of the backscattered electrons increases with increasing atomic number and decreases with increasing beam energy. Both these relationships are nonlinear. In addition, the thickness of the target material influences the scattering, the first layers of the scattering material contributing most to the effect. The general relationship between the quantities which affect backscattering is illustrated in Figure 2 [4]. To explain the experimental backscattering results, Archard [5] proposed a theory which is based on two existing theories, diffusion and large-angle single Rutherford scattering, since only the combination of both offered

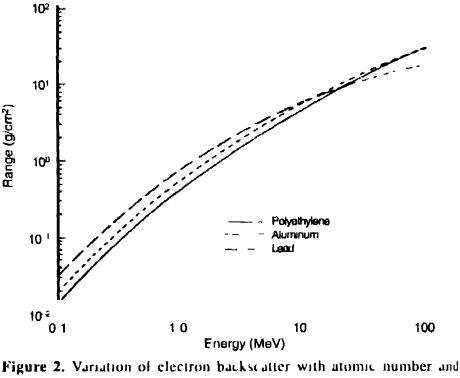

Figure 2. Variation of electron backscatter with atomic number and beam energy.

agreement with experiment. The diffusion and large single elastic scattering involve different mechanisms but are, in this context, regarded as complementary rather than contradictory. These theories predominate for high and low atomic numbers, respectively.

Archard assumed, in his approach, that a beam of electrons suffers, at the beginning of its travel in the medium, collisions with energy losses only, but very little scattering. Thus, it moves in an almost straight line. As the energy decreases with depth, scattering will become more important, until finally the stage of diffusion is reached where the direction of motion becomes completely random. It can be assumed with approximation that there is a direct transition from a 'straight' motion into diffusion.

Bethe [2] defined the depth of penetration X_d corresponding to the transition depth in complete diffusion as the depth at which the average cosine between the actual direction of motion and the direction of the primary beam becomes 1 (angle of 68.4). Archard deduced from this that the ratio of the depth of complete diffusion to the full range X of the electron is $X_d / X_r = 40/7Z$. It follows that in targets of low Z the ratio X_d/X_r is greater than in targets of high Z, and hence, electrons can trav

large distances, having plenty of opportunity for single elastic collisions to take place Under these circumstances, the probability of scattering is low, which results in a low backscatter coefficient In low atomic number materials, the backscattered electrons are therefore the result of multiple Rutherford-type collisions

Everhart [6] deduced a backscattering coefficient for a single elastic scatter collision ·

$$R_s = (a - 1 + 0.5^a)/(a + 1), \quad (8)$$

where

$$a = Z/16 \ln (0.174 V_0/Z) \quad (9)$$

The single elastic backscatter coefficient R is thus given as a function of V_0 and Z. The quantity V_0 represents the energy expressed in volts, $V_0 = E/e$, but the coefficient is almost energy independent. As the atomic number rises, the ratio X_d/X_r falls At high Z, it is small, electrons become diffused almost immediately and the probability for large single elastic scattering is very low Thus, for high Z materials, diffusion is predominant The high probability for multiple collisions increases the number of backscattered electrons capable of escaping from the scatterer, and thus the backscattered coefficient is high for large atomic number scatterers.

Archard [5] deduced for this region, a backscattering coefficient given by $R = (7Z - 80)/(14Z - 80)$ There are, therefore, three domains in the composite theory one in which the diffusion theory predominates (high Z) and a second (low Z) where the Rutherford single scattering predominates In between, there is clearly a transitional region, which is the most difficult to treat theoretically Archard has shown that the experimental data fit reasonably well to the scattering material is concerned The dependence on the electron energy, which was shown to exist in the case of high-energy electrons, was not given consideration in his treatment of backscattering.

As we will be dealing with both metals and biological materials, to unify our approach, an average atomic mass number is defined for biological materials, instead of considering the separate compositions [4].

The elemental composition of body tissues components, the mass attenuation coefficients (or mass stopping powers) in biological materials and the effective atomic numbers in biological materials, for electrons, and photons, with different energies are shown in Tables 1–3, respectively [7]

3. Method of calculation

In this paper, we consider electrons with energy in the range of KeV upto 20 MeV. The essential factors which we need to solve the problem, are : (a) determination of energy lost during scattering event, (b) differential scattering cross section, which characterizes the scattering process and (c) determination of the distance between scattering events

Table 1. Elemental compositions of body tissue components

	H	C	N	O	Na	Mg	P	S	Cl	K	Ca
Bone	3.4	15.5	4.2	43.5	0.1	0.2	10.3	0.3	–	–	22.5
Spleen	10.3	11.3	3.2	74.1	0.1	-	0.3	0.2	0.2	0.3	–
Liver	10.3	15.6	2.7	70.1	0.2	-	0.3	0.3	0.2	0.3	–
Muscle	10.1	17.1	3.6	68.1	0.1	–	0.2	0.3	0.1	0.4	–
Mucin	4.8	34.3	–	60.9	–	–	–	–	–	–	–
Water	11.2	–	–	88.8	–	–	–	–	–	–	–

Table 2. Mass attenuation coefficients or mass stopping powers in biological materials

	1	5	10	20	50 MeV
Bone	1.675	1.896	2.163	2.589	3.735
Muscle	1.870	2.098	2.345	2.721	3.628
Liver	1.875	2.104	2.354	2.731	3.644
Spleen	1.877	2.112	2.366	2.749	3.672
Mucin	1.750	1.950	2.176	2.526	3.393
Water	1.902	2.155	2.420	2.819	3.768

3.1 Collisional loss ·

There is an expression, derived by Bethe [2] which gives the kinetic energy lost by a relativistic electron as it passes through the matter of length dx.

$$-\frac{dT}{dx} = 2\pi N_a r_e^2 m_e c^2 \frac{\rho Z}{A\beta^2}\left[\ln\frac{\tau^2(\tau+2)}{2(I/m_e c^2)^2} + F(\tau)\right]. \quad (10)$$

In the above equation, T is the kinetic energy of the

Table 3. Effective atomic numbers in biological materials, for electrons and photons with different energies

		1	5	10	20	50 MeV
Bone	Photons	6 0	6 3	6 7	7 1	7 5
	Electrons	6 0	6 3	6 4	6 6	6 7
	He ions	5 1	5 4	5 5	5 5	5 5
Muscle	Photons	3 4	3 6	3 8	4 0	4 4
	Electrons	3 5	3 7	3 9	4 1	4 3
	He ions	3 3	3 4	3 2	3 2	3 3
Liver	Photons	3 4	3 6	3 8	4 0	4 3
	Electrons	3 5	3 7	3 9	4 1	4 3
	He ions	3 3	3 4	3 1	3 2	3 3
Spleen	Photons	3 4	3 6	3 8	4 0	4 4
	Electrons	3 5	3 7	3 9	4 1	4 4
	He ions	3 3	3 4	3 2	3 2	3 3
Muein	Photons	4 6	4 7	4 9	5 1	5 3
	Electrons	4 6	5 0	5 1	5 2	5 5
	He ions	4 5	4 6	4 4	4 4	4 4
Water	Photons	3 3	3 5	3 7	4 0	4 3
	Electrons	3 4	3 7	3 9	4 1	4 3
	He ions	3 2	3 3	3 1	3 2	3 2

electron, m_e is the electron rest mass, N_a is the Avogadro number, and Z is the atomic number. A, atomic mass of the target, I, average ionization potential, τ, is the electron energy on $m_e c^2$ unit We have

$$2\pi N_a e_e^2 c^2 = 0\ 1535 \ \text{MeV cm}^2\ \text{gr}^{-} \tag{11}$$

and

$$F(\tau) = 1 - \beta^2 + \frac{\frac{\tau}{8} - (2\tau + 1)\ln 2}{(\tau + 1)^2} \tag{12}$$

3 2 Radiative loss

The loss of energy due to radiation of incident electron with kinetic energy within the limit $m_e c^2 << T << 137 m_e c^2 \cdot^{1/3}$ is [8] .

$$-\frac{dT}{d\lambda} = 4N_a r_e^2 \alpha \frac{\rho Z^2 I'}{A}\left[\ln\frac{2T}{m_e c^2} - 0\ 33 - F(Z)\right] \tag{13}$$

T (MeV) is the kinetic energy of incident electron, and $' = 1/137$, where

$$4N_a r_e^2 \alpha = 0\ 00138 \ \text{MeV cm}^2\ \text{gr}^{-1} \tag{14}$$

and

$$F(Z) = a^2[(1-a^2)^{-1} + 0\ 202 - 0\ 0039a^2 + 0\ 0083a^4 + 0\ 002a^6]. \tag{15}$$

Here, $a = Z/137$

The total energy loss the electron through matter will be as

$$\left(\frac{dT}{dx}\right)_{\text{total}} = \left(\frac{dT}{dx}\right)_{\text{radiation}} + \left(\frac{dT}{dx}\right)_{\text{collision}} \tag{16}$$

3.3 Scattering cross section

For calculating the scattering cross section, we use the screened Rutherford cross section [9], as

$$\frac{d\sigma}{d\Omega} = \frac{Z(Z+1)e^4}{p^2\upsilon^2} \times \frac{1}{(1-\cos\theta + 2B_e)^2} \tag{17}$$

where $B_0 = 0\ 25\left(\frac{1\ 12\lambda_0 h}{p}\right)^2$ and $\lambda_0 = \frac{z^{1/3}}{0\ 885 a_0}$, in which a_0 is the Bohr radius

If we integrate on all of solid angle, we have the total cross section as

$$\sigma_t = \frac{\pi Z(Z+1)e^4}{B_0(1+B_0)p^2\upsilon^2} . \tag{18}$$

3 4 Determination of events interval .

If we assume that the attenuation has an exponential form, the mean free-path of electron is given by

$$\lambda = \frac{1\ 02B_0(1+B_0)AT^2}{Z(Z+1)\rho} \tag{19}$$

where $\rho\left(\text{gr cm}^{-3}\right)$ is the target density

4. Geometrical calculations

Let us consider the path of a typical electron as it moves through the medium and undergoes a succession of scatterings, whereby it changes from some initial direction to some other direction. A typical electron path is illustrated in Figure 3 The extent of its redirection is determined by the magnitudes of the scattering angle θ and the azimuthal angle ϕ We assume that after the electron moves some characteristic distances in a given direction, it encounters a scattering centre The scattering deflects the electron by an angle θ relative to its current direction of travel, with the differential scattering cross section in essence determining θ The azimuthal angle ϕ is assumed to be a uniformly distributed random angle between 0 and 2π rad at each scattering event Since the direction of the velocity of the electron changes at each

scattering event by an amount relative to its current direction, there are clearly two important frames of reference to consider (i) Laboratory frame, which is rigidly attached to the slab Figure 4 is viewed by an observer

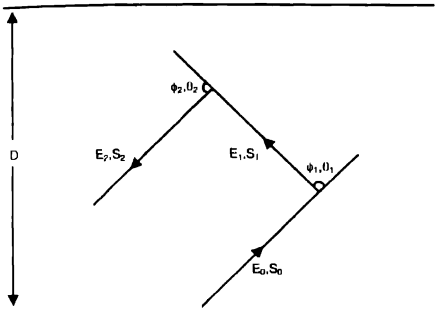

Figure 3 A typical electron path

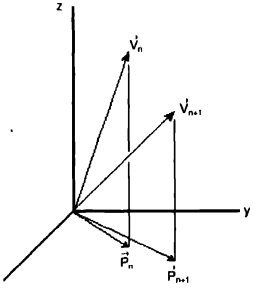

Figure 4 Laboratory frame of reference

sitting in such a frame (ii) Scattering frame which co-moves with the electron This frame undergoes many sudden relative changes in its reference directions. There one such re-orientation after each scattering event Since we are interested in such questions as how many electrons from a given group are transmitted, how many are backscattered, and how many are absorbed by the material, it is most convenient to use the laboratory frame as the fundamental frame of reference, whereas the questions concerning how many electrons cross various material boundaries are simple to answer in the scattering frame, or frame attached to the material, since the medium is at rest

Now, we try to present the geometrical connection between these two frames of reference At a given step, the direction of the electron is defined by a unit vector v_n specified by θ_n, ϕ_n relative to axes fixed to in the laboratory frame. The scattering angles θ and ϕ are defined in the scattering frame which uses v_n to define z' axis. The electron travels in the direction v_n until it undergoes a scattering defined by the scattering angle θ The new direction of the electron in the laboratory frame is defined by the unit vector v_{n+1} Now, we want to find θ_{n+1} and ϕ_{n+1} in terms of θ_n, ϕ_n, θ, and ϕ (the azimuthal scattering angle)

According to Figure 4, we have

$$v_n = \sin\theta_n\cos\phi_n i + \sin\theta_n\sin\phi_n j + \cos\theta_n k, \tag{20}$$

$$v_{n+1} = \sin\theta_{n+1}\cos\phi_{n+1} i + \sin\theta_{n+1}\sin\phi_{n+1} j + \cos\theta_{n+1} k, \tag{21}$$

$$v_{n+1} = \sin\theta\cos\phi i' + \sin\theta\sin\phi j' + \cos\theta k', \tag{22}$$

where i', j', and k' refer to scattering frame of reference We choose to connect the scattering frame (primed) to the laboratory frame (unprimed) as :

$$k' = v_n, \tag{23}$$

$$j' = v_n \times k/|v_n \times k| = v_n \times k/\sin\theta, \tag{24}$$

or

$$J' = \sin\theta_n\, i - \sin\phi_n j, \tag{25}$$

$$i' = j' \times k' = (k - \cos\theta_n v_n)/\sin\theta_n \tag{26}$$

A little algebra then gives

$$v_{n+1}\, k = \cos\theta_{n+1} = \cos\theta_n\cos\theta + \sin\theta_n\sin\theta\cos\phi, \tag{27}$$

$$v_{n+1}\, v_n = \cos\theta = \cos\theta_n\cos\theta_{n+1} + \sin\theta_n \times \sin\theta_{n+1}\cos(\phi_{n+1} - \phi_n), \tag{28}$$

or

$$\cos(\phi_{n+1} - \phi_n) = (\cos\theta - \cos\theta_n\cos\theta_{n+1})/(\sin\theta_n\sin\theta_{n+1}) \tag{29}$$

5. Simulation procedure

For simplicity, we follow one electron through one scattering event. The initial electron's direction of motion is given by v_n (θ_n, ϕ_n) and its kinetic energy is T_n. An elastic scattering event occurs which defines the angles θ and ϕ. The old (θ_n, ϕ_n) and the scattering angles (θ, ϕ) serve to define the direction given by v_{n+1} (θ_{n+1}, ϕ_{n+1}). The electron continues travelling through the target material, ionizing atoms and losing energy for some path length, until it undergoes another elastic scattering.

The normalized probability that the electron scatters through an angle θ is given by :

$$P(\theta) = \frac{1}{\sigma_T}\int_0^{\pi}\int_0^{2\pi} d\Omega\,(d\sigma/d\Omega)$$

$$= \frac{(1+B_0)(1-\cos\theta)}{(1+2B_0-\cos\theta)} \tag{30}$$

Thus,

$$\cos\theta = 1 - \frac{2B_0 P(\theta)}{1+B_0-P(\theta)} \tag{31}$$

Since we consider unpolarized electrons, there is no other direction in space to fix the angle ϕ, hence, it can be any angle between 0 and 2π. In order to generate (θ, ϕ), we now choose two random numbers R_θ and R_ϕ between zero and one. Then θ and ϕ are determined by

$$\cos\theta = 1 - \frac{2B_0 R_\theta}{1+B_0-R_\theta}$$

$$\phi = 2\pi R_\phi \tag{32}$$

The distance the electron travels before having the next elastic collision, can be chosen to be the mean free-path (λ) or by a logarithmic distribution of path lengths. In the logarithmic case, the path-length between collisions is found by assuming an exponential attenuation of the electron beam. If $N(s)$ is the number of electrons which persist after a path-length (s), with initial values $N(0)$, then :

$$N(s) = N(0)\exp(-s/\lambda) \tag{33}$$

The probability that an electron interacts after travelling a distance s is

$$P(s) = [N(0) - N(s)]/N(0) = 1 - \exp(-s/\lambda) \tag{34}$$

Hence,

$$s = -\lambda \ln[1 - P(s)] \tag{35}$$

By choosing a random number (R_s), between 0 and for 1, for $[1 - P(s)]$, since $P(s)$ is between 0 and 1 we can then find a path length (s) travelled by the electron. It means by choosing a random number R_s, we can find the path length travelled by the electron. The energy lost by the electron in each collision is simply taken as $(dT/ds)s$. $\boldsymbol{R}_n$ represents the position vector of the electron in the laboratory frame before the n-th scattering and T_n represents the kinetic energy of the electron for the n-th scattering. The following steps were undertaken in the program :

1st step : given (ϕ_n, θ_n)

2nd step : generate random number $(R_\theta, R\phi, R_s)$.

3rd step : determination of random scattering angles by following relations :

$$s = 2\pi R_\phi, \quad \cos\theta = 1 - \frac{2B_0 R_\theta}{1+B_0-R_\theta}$$

4th step : conversion of scattering frame of reference to Lab frame

$$\cos(\theta_{n+1}) = \cos\theta_n\cos\theta + \sin\theta_n\sin\theta\cos\phi,$$

$$\times \tan(\phi_{n+1} - \phi_n) = \sin\theta_n\sin\theta\sin\phi/$$

$$\times (\cos\theta - \cos\theta_n\cos\theta_{n+1})$$

5th step : determination of next collision point

$$s_n = -\lambda \ln[1 - P(s_n)]$$

$$= -\lambda \ln R_s = \frac{-1.02 B_0(B_0+1)AT_n^{-2}\ln R_s\,(\mu m)}{Z(Z+1)\rho}$$

6th step : $\boldsymbol{R}_{n+1} = \boldsymbol{R}_n + s_n(\sin\theta_{n+1}\cos\phi_{n+1}\hat{i}$

$$+ \sin\theta_{n+1}\sin\phi_{n+1}\hat{j} + \sin\theta_{n+1}\hat{k}$$

7th step : $T_{n+1} = T_n -$

8th step : $\theta_{n+1} \to \theta_n$; $\phi_{n+1} \to \phi_n$

9th step : check the following conditions

(a) Is electron transmitted? If yes, increment $N_{\text{transmitted}}$ by one and go to next electron, $N_{\text{trans}} \leftarrow N_{\text{trans}} + 1$,

(b) is electron backscattered across material boundary? If yes, increment $N_{\text{backscatter}}$ by one and go to next electron $\left(N_{\text{backscatt}} \leftarrow N_{\text{backscatt}} + 1\right)$

(c) Is electron kinetic energy less than 0.5 keV? If yes, increment N_{absorbed} by one and go to next electron, $\left(N_{\text{absorp}} \leftarrow N_{\text{absorp}} + 1\right)$

(d) If none of these checks are passed, then go to (1st) step.

10th step : when all electrons have been followed, compute :

R = number backscattered electrons/number of incident electrons.

T = number of transmitted electrons/number of incident electrons

A = number of absorbed electrons/number of incident electrons

5. Results and discussion

The procedure explained in Section 4 was employed for

the transport of electrons (of different energies and incidence angles) through different solids and biological materials (of different types and thicknesses)

In Figure 5, the tracks of 10 electrons of 8 MeV energy passing through Aluminium at 45 degree incidence angle are shown In Figures 5 and 6, the same energy

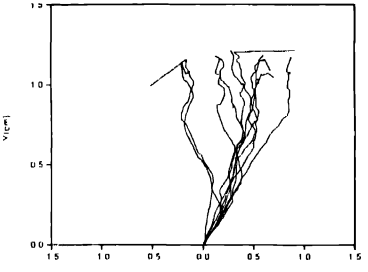

Figure 5 Ten tracks of 10 electrons passing through Al at 45 degree incidental angle

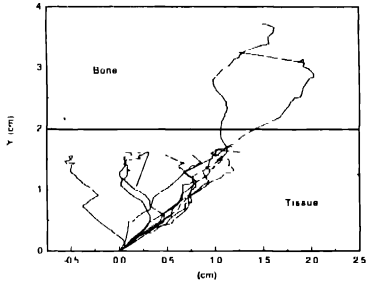

Figure 6 Ten tracks of 10 MeV electrons passing through tissue to bone at 45 degree incidental angle.

electrons were tracked while passing through bone-tissue interface

The tracks given in Figures 5 and 6 are qualitatively well-compatible with those published by Williamson *et al* [10] and also they are quantitatively in agreement with the calculations made by *N*-particle transport Monte Carlo code, MCNP [11], as shown in Figure 7.

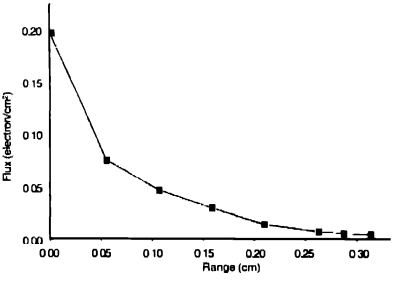

Figure 7. Penetration depth of 8 MeV electrons through Aluminium using MCNP

Figure 8 shows the ionization curve (or equivalently the relative absorbed dose (%)) of 8 MeV electrons produced by the Linear Electron Accelerator of Radiotherapy division of Imam Reza Hospital, through water *versus* depth (mm) The procedure of electron transport explained in Section 4 was also employed for this case The overall agreement, as listed in Table 4, with both data from Thirumala *et al* [12], MCNP code and experimental results of Imam Reza

Hospital electron LINAC is acceptable due to the relatively small relative errors

Table 4. Energies and ranges of electrons in different materials

Material	Mean range (cm) Imam Reza Electron accelerator	Mean range (cm) MCNP results	Mean range (cm) Ref [12]	Mean range (cm) Monte Carlo method (This work)	Energy (MeV)
Water			5 55	5 5 (0 9%*)	12
Water	4 8		4 5	4 5 (6 25%)	10
Water	4 1			3 8 (7 32%)	8
Aluminium		2 1		1 9 (10.5%)	12
Aluminium			1 9	1 7 (10 5%)	10
Aluminium				1 2	8
Lead				1 35	12
Lead		0 35	0 5	0 33 (34%)	10
Lead		0 3		0 25 (16 6%)	8

* The maximum relative error of the Monte Carlo results compared with those in Ref [12], MCNP calculations and experiments undertaken at Imam Reza Hospital

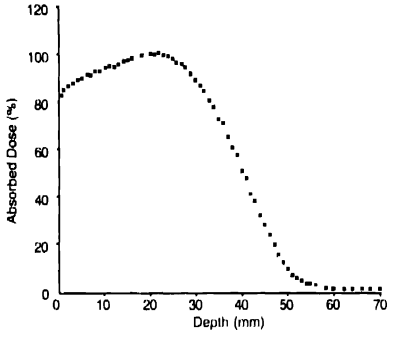

Figure 8. Relative absorbed dose (%) of 8 MeV electrons passing through water, at zero degree incident angle, versus depth (mm), which indicates an equivalent range of 4 cm in water

Acknowledgment

We would like to thank the technical staff of Imam Reza Hospital of Mashhad, Iran, for invaluable help and cooperation

References

[1] I M A Sobol *A Premier for the Monte Carlo Method* (Boca Raton, FL CRC Press) (1994)

[2] H A Bethe *Ann Phys* **5** 325 (1930)

[3] S M Seltzer and M J Berger *Intl J Appl Rad. Isot* **33** 1219 (1982)

[4] S C Klevenhagen *Physics of Electron Beam Therapy* (Bristol Adam-Hilger) (1985)

[5] G D Archard *Proc Phys Soc* **74** 177 (1959)

[6] T E Everhart *J Appl Phys* **31** 1483 (1960)

[7] K Pathasaradhi, B Mallikarjuna and S Guru Prasad *Med Phys* **16** (1989)

[8] G F Knoll *Radiation Detection and Measurement* (New York John Wiley) (1989)

[9] W R Leo *Techniques for Nuclear and Particle Physics Experiments* (New York Springer-Verlag) (1987)

[10] W Williamson and G C Duncan *Am J Phys* **54** 262 (1986)

[11] John S Hendricks, K J Adams, T E Booth, J F Briesmeister, L L Carter, L J Cox, J A Favorite, R A Forster, G W McKinney and R E Prael *Appl Rad Isot* **53** 857 (2000)

[12] B V Thirumala Rao, M L N Raju, K L Narasimham, K Parthasaradhi and B Mallikarjuna *Rao Med Phys* **12** 745 (1985)